Article

Deep Neural Network Assisted Quantum Chemistry Calculations on Quantum Computers

Kalpak Ghosh, Sumit Kumar, Nirmal Mammavalappil Rajan, and Sharma S. R. K. C. Yamijala*

Read Online

ACCESS | Metrics & More | Article Recommendations | Supporting Information

ABSTRACT: The variational quantum eigensolver (VQE) is a widely employed method to solve electronic structure problems in the current noisy intermediate-scale quantum (NISQ) devices. However, due to inherent noise in the NISQ devices, VQE results on NISQ devices often deviate significantly from the results obtained on noiseless statevector simulators or traditional classical computers. The iterative nature of VQE further amplifies the errors in each loop. Recent works have explored ways to integrate deep neural networks (DNN) with VQE to mitigate iterative errors, albeit primarily limited to the noiseless statevector simulators. In this work, we trained DNN models across various quantum circuits and examined the potential of two DNN-VQE approaches, DNN1 and DNNF, for predicting the ground state energies of small molecules in the presence of device noise. We carefully examined the accuracy of the DNN1, DNNF, and VQE methods on both noisy simulators and real quantum devices by considering different ansatzes of varying qubit counts and circuit depths. Our results illustrate the advantages and limitations of both VQE and DNN-VQE approaches. Notably, both DNN1 and DNNF methods consistently outperform the standard VQE method in providing more accurate ground state energies in noisy environments. However, despite being more accurate than VQE, the energies predicted using these methods on real quantum hardware remain meaningful only at reasonable circuit depths (depth = 15, gates = 21). At higher depths (depth = 83, gates = 112), they deviate significantly from the exact results. Additionally, we find that DNNF does not offer any notable advantage over VQE in terms of speed. Consequently, our study recommends DNN1 as the preferred method for obtaining quick and accurate ground state energies of molecules on current quantum hardware, particularly for quantum circuits with lower depth and fewer qubits.
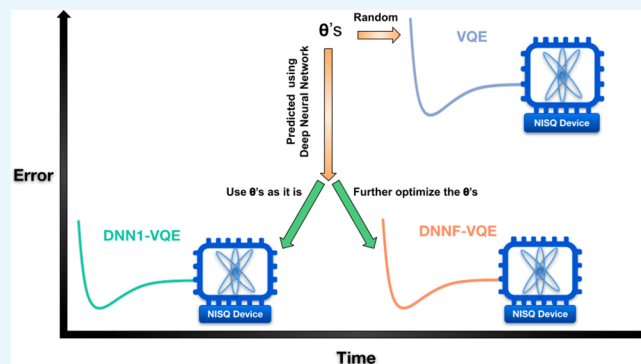
■ INTRODUCTION

The development of quantum computing has provided a new avenue for studying the electronic structure of molecules and materials.[1−9] A variety of quantum algorithms have been developed to solve electronic structure problems by harnessing quantum phenomena such as superposition and entanglement on a quantum computer.[1,10−12] Among these algorithms, the variational quantum eigensolver (VQE) is the most commonly used algorithm to solve electronic structure problems on the current noisy intermediate-scale quantum (NISQ) computers.[4,13−17] In this context, one of the major uses of VQE is to calculate the ground state energies of molecules.

To solve the electronic structure problem of a molecule on a classical computer, one writes the Hamiltonian operator in the second quantized representation, i.e., in terms of the Fermionic creation $(a_i^\dagger)$ and annihilation (a_i) operators as

$$\hat{H} = \sum_{p,q} h_{pq} a_p^\dagger a_q + \frac{1}{2} \sum_{p,q,r,s} h_{pqrs} a_p^\dagger a_q^\dagger a_r a_s \quad (1)$$

where h_{pq} and h_{pqrs} are the one and two-electron integrals, respectively. On a quantum computer, the Fermionic

Hamiltonian has to be mapped onto a qubit Hamiltonian, where the Fermionic operators are converted into qubit operators (the familiar Pauli matrices/gates) through any of the several Fermion to qubit mapping schemes such as Jordan-Wigner mapping, parity mapping, Bravyi-Kitaev mapping, etc.[18−20] It is important to note that the Pauli matrices are the native operators (gates) on a quantum computer.

Apart from the Hamiltonian, we also need to represent the wave function, $\Psi(\theta)$, of the molecule on a quantum computer, and this is done using a variety of parametrized quantum circuits, also known as ansatzes. An ansatz, $\Psi(\theta)$, can be represented as

$$|\Psi(\theta)\rangle = \hat{U}(\theta)|\Psi_0\rangle \quad (2)$$

where $\hat{U}(\boldsymbol{\theta})$ is a unitary operator that is parameter-dependent, and Ψ_0 is the reference wave function, which is often taken as the Hartree–Fock (HF) wave function. Depending on the unitary operator that we operate on the initial reference state, a variety of ansatzes can be created, and one popular ansatz is the "unitary coupled cluster" (UCC) ansatz, $\Psi_{UCC}(\theta)$.[1,16,21] To create a UCC ansatz, the reference wave function, Ψ_0, is operated with a UCC operator, which can be written as

$$\hat{U}(\boldsymbol{\theta}) = e^{(T(\boldsymbol{\theta}) - T(\boldsymbol{\theta})^{\dagger})} \qquad (3)$$

where $T(\boldsymbol{\theta})$ is the cluster operator, which can be written in the second quantized notation as the sum of singles, doubles, and other higher-level excitation operators, i.e., $T(\boldsymbol{\theta}) = T_1(\boldsymbol{\theta}) + T_2(\boldsymbol{\theta}) + ...$, where, $T_1(\boldsymbol{\theta})$ and $T_2(\boldsymbol{\theta})$ are the single and double excitation cluster operators, respectively, with the operator forms

$$T_1(\boldsymbol{\theta}) = \sum_{\substack{i \in occ \\ a \in virt}} \theta_{ia} a_a^{\dagger} a_i; \qquad T_2(\boldsymbol{\theta}) = \sum_{\substack{i,j \in occ \\ a,b \in virt}} \theta_{ijab} a_a^{\dagger} a_b^{\dagger} a_i a_j \qquad (4)$$

Here, θ_{ia} and θ_{ijab} are the rotational angles that can be tuned to obtain the ground state wave function, for example, variationally. By truncating the $T(\boldsymbol{\theta})$ at the singles and doubles excitations, one obtains the unitary coupled cluster singles and doubles (UCCSD) ansatz, $\Psi_{UCCSD}(\boldsymbol{\theta})$, a commonly employed ansatz in the quantum chemistry calculations, including this work. Here, the UCCSD operator is given by

$$\hat{U}(\boldsymbol{\theta}) = e^{(T_1(\boldsymbol{\theta}) - T_1(\boldsymbol{\theta})^{\dagger}) + (T_2(\boldsymbol{\theta}) - T_2(\boldsymbol{\theta})^{\dagger})} \qquad (5)$$

Since any operation on a gate-based quantum computer is done through one- and two-qubit gates, the UCCSD operator also has to be decomposed into one- and two-qubit gates. This decomposition is performed using the Trotter-Suzuki approximation,[22,23] where the exponential sum of the operators in eq 5 (R.H.S.) is decomposed into a product of exponential operators (R.H.S. of eq 6).

$$\hat{U}(\boldsymbol{\theta}) = \lim_{n \to \infty} \left(e^{\frac{(T_1(\boldsymbol{\theta}) - T_1(\boldsymbol{\theta}^{\dagger}))}{n}} e^{\frac{(T_2(\boldsymbol{\theta}) - T_2(\boldsymbol{\theta}^{\dagger}))}{n}} \right)^n \qquad (6)$$

In general, the above approximation is exact in the infinite order; i.e., a large number of steps, n, are necessary to decompose the UCCSD operator accurately. However, such a large number of Trotter steps would lead to extremely deep quantum circuits. Since one of the main objectives of this work is to perform calculations on real quantum devices, quantum circuits that are as shallow as possible are required. For this reason, in this work, a single Trotter step is used. Under this approximation, the UCCSD operator can be written as

$$\hat{U}(\boldsymbol{\theta}) \approx e^{(T_1(\boldsymbol{\theta}) - T_1(\boldsymbol{\theta})^{\dagger})} e^{(T_2(\boldsymbol{\theta}) - T_2(\boldsymbol{\theta})^{\dagger})} \qquad (7)$$

It is important to note that earlier works by Barkoutsos et al. and Romero et al. have specifically shown that the ground state energy of small molecules like H_2 and LiH molecules (which are considered in this work) can be accurately obtained even when expanding the wave function with a single Trotter step.[15,24]

By knowing the Hamiltonian and wave function of a molecule, the energy expectation value can be computed on a quantum computer within the VQE approach as

$$E = \min_{\boldsymbol{\theta}} \langle \Psi(\boldsymbol{\theta}) | \hat{H} | \Psi(\boldsymbol{\theta}) \rangle \qquad (8)$$

Here, following the variational principle, the parameters ($\boldsymbol{\theta}$) of the ansatz are updated iteratively on a classical computer until the ground state energy of the molecule is converged.

One of the primary applications of quantum chemistry is to understand reaction mechanisms. Since a reaction typically involves the breaking and making of bonds, the knowledge of molecular energies at various geometries (i.e., constructing a potential energy surface (PES)) is crucial in finding the reaction mechanism. Accordingly, for constructing a PES using the VQE algorithm, ground state energy calculations have to be carried out for multiple molecular geometries. However, such a task on the current NISQ devices is difficult due to the combined limitations of both quantum devices and the VQE algorithm. The current quantum devices are limited in both the number and the quality of qubits and, more importantly, the fidelity of quantum gates that are applied onto the qubits.[25] Similarly, the efficiency of the VQE algorithm is dependent on the quality of the ansatz and the optimization of the circuit parameters. The ansatz has to be expressive enough to capture the correlations in the molecule, and at the same time, the circuit depth has to be shallow enough such that it is tractable on a quantum computer.[1,11] Moreover, while simulating larger molecules, optimization of the circuit parameters is often a daunting task due to the large number of parameters involved in the ansatz.[26–28] There have been significant efforts to improve the quality of the quantum hardware and quantum algorithms.

Recent works have proposed novel ways to improve the efficiency of the VQE algorithm, such as (i) proposing newer chemically inspired ansatzes like k-UpCCGSD with lower circuit depths than that of the UCCSD ansatz,[29] (ii) modifying the existing UCCSD ansatz through operator screening or by using the newer variants of UCCSD like dual exponential variant for reducing the circuit depth,[30–32] and (iii) by employing embedding schemes and entanglement forging techniques for reducing the qubit requirement while working with larger molecules.[33,34] Specific to the issue with the parameter optimization in VQE, Tao et al. proposed the deep neural network (DNN)-VQE method, where a DNN model is used to predict the final optimized variational parameters for the quantum circuit.[35] Using such parameters as the initial point for a VQE calculation, the authors showed that the DNN-VQE method is able to accurately construct the PESs of several small molecules such as H_2, LiH, BeH_2, and H_4. However, unfortunately, these simulations are not performed on real quantum devices. Also, these simulations did not include any hardware noise (which can be emulated on simulators). As such, although the DNN-VQE results are quite promising, their applicability for real quantum devices is yet to be explored.

In this work, we studied the potential of the DNN-VQE method in both the presence and absence of noise. To this end, we studied both LiH and H_2 molecules on the *ibmq_qasm_simulator* with the noise model of IBM's *ibm_brisbane* quantum computer. More importantly, by varying qubit counts and circuit depths, we conducted several quantum chemical simulations on the real quantum hardware (*ibm_brisbane* device) to identify the true advantages of DNN-VQE over VQE. Our results indicate that the DNN-VQE is consistently superior to VQE in predicting the ground state energies of molecules in both the presence and absence of noise. However, we also find that the DNN-VQE is practically
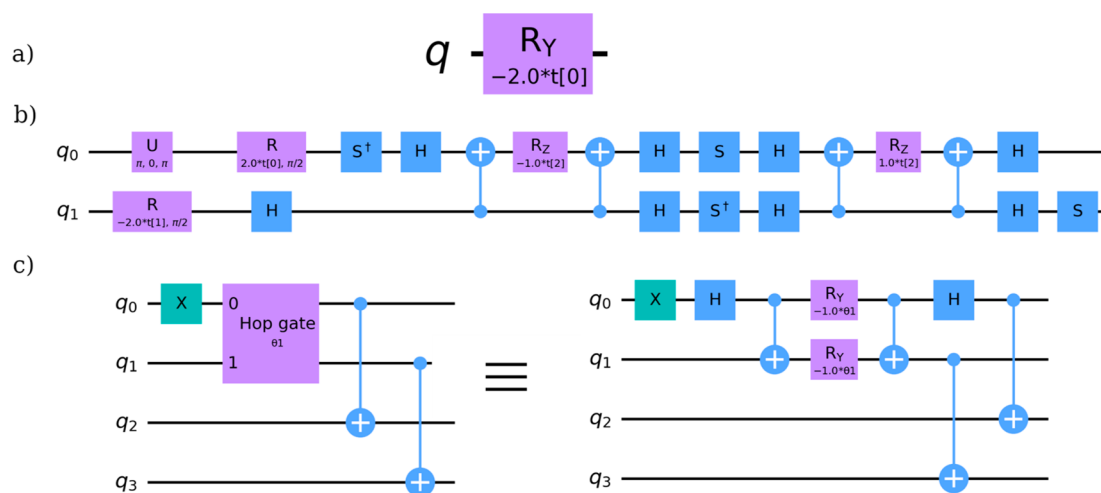
Figure 1. Quantum circuits (ansatzes) of various depths and qubit counts for representing the wave function of an H_2 molecule on a quantum computer. (a) one-qubit UCCSD ansatz, (b) two-qubit UCCSD ansatz, and (c) four-qubit Givens ansatz. Figure S3 depicts a four-qubit UCCSD ansatz. Additional details of all of these quantum circuits are provided in Table S1.

useful only for quantum systems with lower circuit depths and fewer qubits.

COMPUTATIONAL DETAILS

We used IBM's Qiskit for all our calculations.[36] The second quantized Hamiltonian and the one and two-electron integrals were obtained using the PySCF package (as interfaced with Qiskit).[37,36] For computing the ground state energies of the molecules using the VQE algorithm, the UCCSD ansatz along with the STO-3G basis set was used.[14,38] For the UCCSD operator, a single Trotter step was considered. Jordan-Wigner mapping was used to transform both the Fermionic Hamiltonian and the UCCSD operator into their corresponding qubit forms. Additionally, for reducing the qubit count, parity mapping and Z_2 symmetries were used, which resulted in ansatzes of different depths and qubit counts. Further, for each of these different ansatzes, the mapomatic package was used to select the best qubits available on the quantum device,[36,39] and the quantum circuits were transpiled at the optimization level 3 using the Qiskit IBM Runtime service.[36] During all the VQE calculations (i.e., both on simulators as well as quantum hardware), the limited-memory Broyden-Fletcher-Goldfarb-Shannon Bound (L-BFGS_B) was used as the optimizer, and four thousand "shots" (where shots represent the number of times a specific quantum circuit is measured) were used. The initial guess parameters for the VQE algorithm were chosen randomly in all cases except for the LiH molecule. For this case, VQE calculations on a statevector simulator with random initial parameters exhibited higher deviations from the CCSD results compared to the VQE calculations, where all the initial parameters were set to zero (Figure S1). To access the *ibmq_qasm_simulator* and the *ibm_brisbane* quantum device, we used the Qiskit IBM Runtime service via version 0.10.0 of the qiskit-ibm-runtime package. For training the DNN models to predict the variational parameters, we closely followed Tao et al.'s work.[35] Briefly, the neural network construction and training were done using TensorFlow.[40] ReLU activation function is used for all the nodes in the neural network, Adam optimizer for training the parameters, and mean absolute percentage error (MAPE) is used as the loss function during model

training.[41] The layout of the DNN model is shown in Figure S2.

RESULTS AND DISCUSSION

Ansatz Preparation. We begin our discussion with the preparation of the UCCSD ansatz for the H_2 and LiH molecules in the STO-3G basis. An H_2 molecule in the STO-3G basis set yields four molecular spin-orbitals, and if we are using the Jordan-Wigner (JW) mapping to represent the wave function on a quantum computer, then every molecular spin-orbital is mapped onto a qubit. Accordingly, we need four qubits to represent a H_2 molecule. However, this qubit count can be further reduced by using other mapping techniques. For example, to reduce it to a two-qubit problem, we can follow the approach of Bravyi et al., where parity mapping is used to reduce the four-qubit problem to a two-qubit one. Similarly, to further reduce it to a one-qubit problem, Z_2 symmetries can be invoked, which tapers off another qubit.[42,43] Thus, the H_2 molecule can be studied with either four or two or one qubit circuits, and accordingly, we can generate different ansatzes. Similarly, to represent the wave function of an LiH molecule on a quantum computer with the STO-3G basis and by considering the JW mapping, we need 12 qubits. However, by considering the parity mapping and Z_2 symmetries, and by freezing the two lowest occupied spin orbitals, the wave function can be represented using six qubits.

For a one-qubit circuit of the H_2 molecule, the UCCSD ansatz consists of only a single R_y gate and one variational parameter (see Figure 1a). However, as we move toward the two- and four-qubit circuits, the UCCSD ansatz yields complex quantum circuits with multiple variational parameters and gates (of various kinds). For example, although the four-qubit UCCSD ansatz has three variational parameters, it yields a quantum circuit of depth 83 (i.e., the largest number of gates acting on any of the four qubits) and size 112 (total number of gates in the circuit). Similarly, for the LiH molecule, the six-qubit UCCSD ansatz gives a quantum circuit of depth 482 and size 858 along with 10 variational parameters, which is even difficult to comprehend! Additional details on these quantum circuits are provided in Table S1, and the quantum circuit diagrams of the two and four-qubit UCCSD ansatzes of the H_2

molecule are presented in Figure 1b and Figure S3, respectively.

It is important to note that the complexity of the large-qubit circuits can be substantially reduced by considering ansatzes that are different from the UCCSD ansatz. Below we provided an alternative heuristic ansatz for the H_2 molecule based on Givens rotation formalism. Using the Givens rotation formalism, a two-qubit hop gate can be created, which transfers/excites an electron from one spin-orbital to another.[44] Effectively, the two-qubit hop gate creates a single excitation on the Hartree−Fock state. Further, the application of CNOT gates between spin-up (control) and spin-down (target) qubits subsequent to the application of a two-qubit hop gate would result in a circuit that generates double excitation on the Hartree-Fock state.[34,45] Such a circuit can capture all of the dominant excitations present in the UCCSD circuit of H_2 but with far less complexity, as shown in Figure 1c. In the subsequent sections, we refer to this circuit as the "four-qubit Givens circuit,", and it is used to study the effect of circuit depth and size on the accuracy of the VQE and DNN-VQE energy predictions.

DNN Models. Next, for each of the circuits presented above, we trained the DNN models. The training and testing data sets consist of a set of bond distances (either H−H or Li−H bond length) and their corresponding statevector-optimized variational parameter(s). Here, the term "statevector-optimized variational parameters" refers to the $\boldsymbol{\theta}$s that are obtained at the last iteration of a VQE algorithm on a *statevector* simulator, and which yield the ground state energy of the molecule at a specific bond length. It is important to note that since the same molecule can be represented using different ansatzes (different number of qubits, gates, and $\boldsymbol{\theta}$s), the DNN models have to be trained separately for each such ansatz. As per the convention, the DNN model is considered to be trained once it accurately predicts the variational parameters for the test set. The trained DNN model can be used to predict the optimal variational parameter(s) for bond distances that are not part of the training and testing data sets.

In this work, using the DNN-predicted parameters, we computed the ground state energies of molecules through two different approaches. In the first approach, the predicted parameters are considered as the final optimized parameters obtained from the VQE algorithm, and the ground state energy is computed directly by using these parameters (i.e., in a single step). We labeled this approach as "DNN1". In the second approach, the predicted parameters are taken as the initial guess parameters for the VQE calculation (instead of taking the random parameters), and the ground state energy is computed after optimizing these parameters (as is usually done in the VQE algorithm). We labeled the second approach as "DNNF". In the subsequent sections, the results from both of these approaches are compared against the VQE results obtained on both noisy simulators as well as on quantum devices.

Validation of the DNN Models. Before presenting the DNN1, DNNF, and VQE results obtained on the *ibmq_qasm_simulator* and the *ibm_brisbane* quantum device, we would like to demonstrate the accuracy of our DNN models on the noise-free statevector simulator. To this end, we computed the ground state energies of H_2 (one-qubit circuit) and LiH (six-qubit circuit) molecules using the DNN1, DNNF, and VQE methods on the statevector simulator, and these results are presented in Figure 2. To validate the accuracy of these
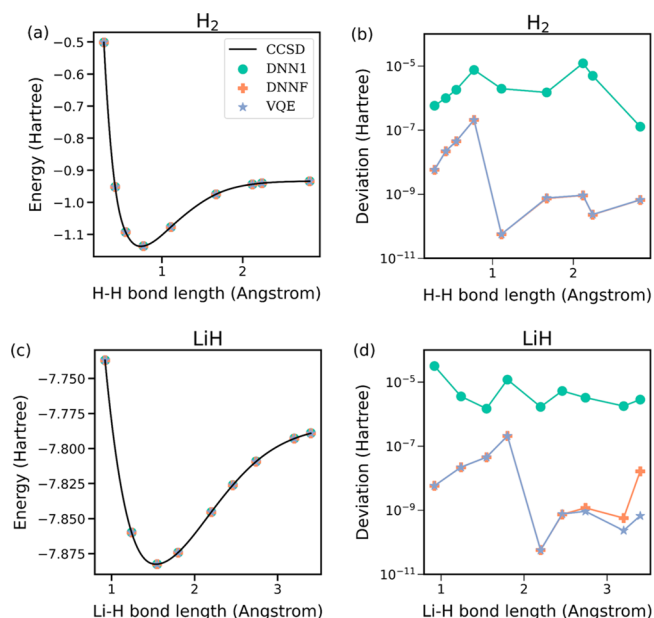

Figure 2. Ground state potential energy surfaces of (a) H_2 and (c) LiH molecules computed using the DNN1, DNNF, VQE, and CCSD methods. Panels b and d depict the deviation in the DNN1, DNNF, and VQE predicted energies (computed on a statevector simulator) from the CCSD energies for H_2 and LiH molecules, respectively. The black solid line represents the CCSD results. The green circle, orange cross, and blue star represent the DNN1, DNNF, and VQE energies, respectively.

results, we compared them against the results obtained using the coupled cluster singles and doubles (CCSD) method on a classical computer. Here, we chose CCSD as our reference state since most of our VQE calculations are with the UCCSD ansatz. Moreover, UCCSD is the unitary form of the CCSD, making it a fair comparison. Also, we chose one-qubit and six-qubit circuits for H_2 and LiH molecules, respectively, since they correspond to the quantum circuits with the smallest qubit counts for these molecules without affecting the accuracy, as shown below.

As depicted in Figure 2 panels a and c, the potential energy surfaces (PESs) of the H_2 and LiH molecules predicted using the DNN1, DNNF, and VQE methods align perfectly with the CCSD results. Furthermore, as presented in Figure 2b,d, for both H_2 and LiH molecules, the deviations in the energies associated with the DNNF and VQE methods from the CCSD are in the order of 10^{-10} to 10^{-7} hartree, indicating their high accuracy. Interestingly, even the DNN1 approach (which does not include any parameter optimization) shows a maximum deviation of only 10^{-5} (10^{-4}) hartree for the H_2 (LiH) molecule, which is well within the limit of chemical accuracy (1.6 millihartree) and demonstrates that the energies predicted using DNN1 are also quite accurate. Here, between DNN1 and DNNF, the latter approach provides more accurate ground state energies, since it includes further optimization of the DNN predicted parameters, which is absent in the former approach. For the same reason, DNNF and VQE results deviate similarly from the CCSD results on a statevector simulator. Together, these results not only validate our DNN models but also demonstrate the suitability of employing both the DNN1 and DNNF methods for predicting the accurate ground state energies of molecules.

Accuracy of the DNN Models on Noisy Simulators. Motivated by the accurate energy predictions of the DNN1, DNNF, and VQE on a statevector simulator, we repeated the ground state energy calculations of H_2 and LiH molecules on the *ibmq_qasm_simulator* by incorporating the device noise of the *ibm_brisbane* device. To account for the statistical noise, we used four thousand shots (i.e., we measured the quantum circuit 4,000 times), and our choice for the number of shots is explained later. Further, to improve the accuracy of the predictions, we also applied the "twirled readout error extinction," T-REx, error mitigation scheme as implemented in the Qiskit.[46] As mentioned earlier, for these calculations, we used the single-qubit and six-qubit UCCSD ansatzes for the H_2 and LiH molecules, respectively. It is worth highlighting that running simulations for the LiH molecule using the DNNF or VQE methods on the *ibmq_qasm_simulator* demands significant computational resources due to the large circuit depths. For example, for each LiH bond length, it takes about *four to five days* to compute the ground state energy. On the contrary, the DNN1 calculations only take ~20−30 min for each LiH bond length. Also, the DNNF and VQE calculations using the single-qubit UCCSD ansatz for the H_2 molecule take about 15−20 min (see Table S2).

In Figure 3a, we show the deviations in the ground state energies as predicted by the DNN1, DNNF, and VQE
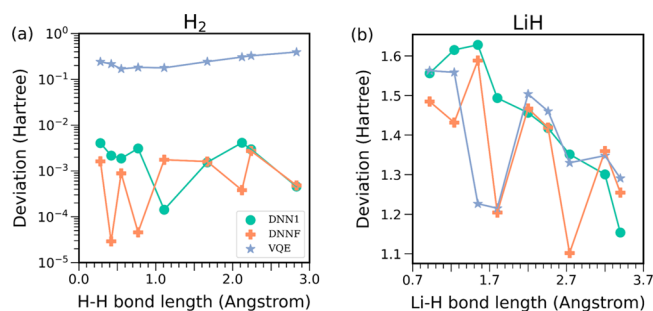

Figure 3. Deviations in the ground state energies predicted using the DNN1, DNNF, and VQE methods from the CCSD energies for (a) H_2 and (b) LiH molecules. The DNN1, DNNF, and VQE calculations were performed on an *ibmq_qasm_simulator* by considering the *ibm_brisbane* device noise, T-REx error mitigation scheme, and four thousand shots.

methods when compared with the CCSD results for the H_2 molecule. Notably, the inclusion of device noise introduced

significant errors in predicting the ground state energies of the H_2 molecule when compared to the statevector results (Figure 2b). With noise, both the DNN1 and DNNF energies deviate by 1×10^{-4} to 1×10^{-2} hartree, whereas VQE energies deviate by 1×10^{-1} hartree from the CCSD results. Clearly, the DNN-predicted variational parameters are helping in achieving superior accuracy when compared to the random initial parameters that are used in the standard VQE calculations. For some bond distances, the energies even meet the limit of chemical accuracy of 1.6 millihartree. Although DNNF generally predicts more accurate energies than DNN1, it is not universally maintained for all bond distances. Together, from these results, it can be inferred that in the presence of device noise, both DNN1 and DNNF provide superior accuracy compared to the standard VQE method.

Considering the success of the DNN1 and DNNF methods in predicting the ground state energies of the H_2 molecule even in the presence of device noise, we extended our analysis to the LiH molecule, and the results are illustrated in Figure 3b. Similar to the H_2 case, the VQE predicted energies for the LiH molecule also deviate from the CCSD results, albeit with significant deviations of more than 1 hartree! Surprisingly, the energies predicted by the DNN1 and DNNF methods also deviate by about 1 hartree for the LiH molecule, even after applying T-REx error mitigation. Such a large deviation from the CCSD results makes the DNN1, DNNF, and VQE results essentially meaningless! Therefore, it is crucial to (i) identify the factors that are responsible for these large deviations, (ii) understand their contributions to the errors, and (iii) where possible find ways to mitigate the errors. Below, we studied the role of three important factors, namely, the circuit depth, the qubit count, and the shot count toward the errors.

Effect of Circuit Depth and Qubit Count on the Accuracy of DNN-VQE approaches. To assess the impact of the qubit count and circuit depth on the accuracy of DNN1 and DNNF approaches on noisy quantum simulators, we considered the two- and four-qubit UCCSD circuits of the H_2 molecule. These circuits exhibit progressively increasing circuit depth compared to that of the one-qubit case (see Table S1). For these new circuits, we retrained our DNN models and once again demonstrated that the energies provided by the DNN1 and DNNF methods on a statevector simulator are very close to the CCSD results, with deviations far below the chemical accuracy (see Figure S4a,b). As such, these results establish that both the DNN1 and DNNF methods will always
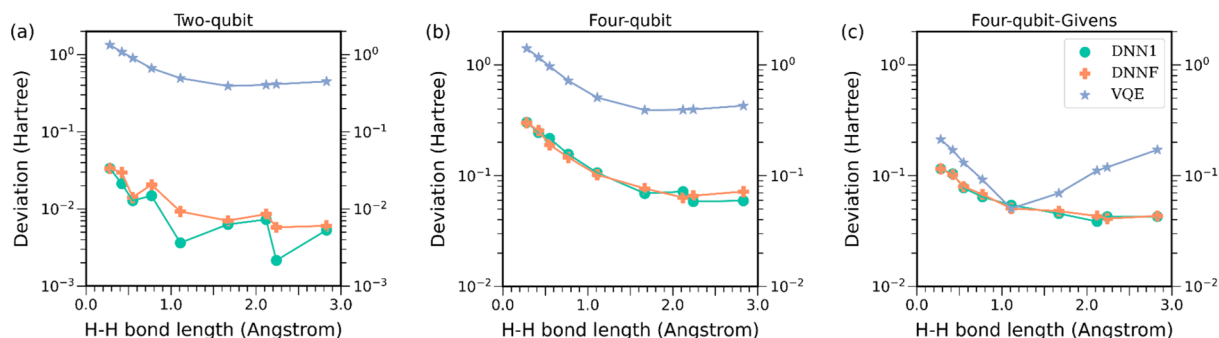

Figure 4. Deviation in the DNN1, DNNF, and VQE predicted energies from the CCSD energy for an H_2 molecule represented using (a) two-qubit UCCSD, (b) four-qubit UCCSD, and (c) four-qubit Givens circuit. The DNN1, DNNF, and VQE simulations were performed using an *ibmq_qasm_simulator* with *ibm_brisbane* device noise, T-REx error mitigation, and four thousand shots. Please note that the y-axis in panels b and c starts from 10^{-2} hartree.

provide accurate results on a statevector simulator irrespective of the qubit count and circuit depth, but their accuracy on noisy devices needs to be further investigated.

Next, we repeated these simulations on the *ibmq_qasm_simulator* by considering the *ibm_brisbane* device noise, T-REx error mitigation scheme, and four thousand shots (hereafter, simply referred to as *noisy simulator*). As depicted in Figure 4a, for the two-qubit circuit, the errors for the DNN1 and DNNF are approximately an order of magnitude higher (ranging from 10^{-3} to 10^{-1} hartree) than those for the one-qubit case (see Figure 3a). Surprisingly, the VQE energies deviate considerably more from the CCSD results, and the errors are on the order of 10^{-1} to 10^0 hartree. For the four-qubit circuit (see Figure 4b), the DNN1 and DNNF predicted energies showed substantial deviations from the CCSD results, with errors in the order of 0.05−0.3 hartree, and the VQE results deviated even further (0.4−1.4 hartree). Therefore, these results clearly prove that, even on noisy simulators, the DNN1 and DNNF methods provide significantly more accurate energies than the VQE. However, the DNN methods would also provide less meaningful results with an increase in the qubit count and circuit depth, as proved here for the case of an H_2 molecule. Similar conclusions can be drawn by comparing the results of different molecules, as well. For example, considering the results of H_2 and LiH (Figure 3) and their circuit depths (Table S1), it can be immediately identified that the substantial circuit depth (482) and larger qubit count (6) of the LiH's UCCSD ansatz plays a prominent role in reducing the accuracy of the DNN1 and DNNF predicted energies for the LiH molecule on a noisy quantum simulator.

Notably, in the above calculations, while moving from a two-qubit circuit to a four-qubit circuit of the H_2 molecule, there is a simultaneous increase in the qubit count and circuit depth. Therefore, to specifically understand the effect of each of these parameters separately, we need to design ansatzes with either the same number of qubits or the same circuit depth. Since fixing the qubit count is easier than fixing the circuit depth, we constructed a heuristic "four-qubit Givens ansatz" for the H_2 molecule, which has a depth (depth = 7) lower than that of the four-qubit UCCSD ansatz (depth = 83). For this new circuit, we first conducted the statevector VQE calculations and retrained the DNN models. Once again, we find that VQE, DNN1, and DNNF provide extremely accurate results on a statevector simulator (Figure S4c), with deviations in the range of 10^{-11} to 10^{-7} hartree from the CCSD energy. Next, we repeated the calculations with the *noisy simulator*. As shown in Figure 4c, the reduced circuit depth of the Givens circuit resulted in a notable improvement in the energies predicted using the VQE, DNN1, and DNNF methods. For example, with the Givens circuit, the maximum deviation in the DNN1 and DNNF predicted energies has reduced to 0.1 hartree, which is a 66% reduction in error compared to the UCCSD circuit. Interestingly, the VQE results for the Givens circuit showed a significant improvement (up to 1.2 hartree, which is about 85% improvement) over the UCCSD circuit. Together, these results suggest that, on a noisy simulator, for the same qubit count, the accuracy of the DNN1, DNNF, and VQE methods can be greatly enhanced by designing lower-depth circuits.

It is crucial to note that generally, VQE calculations are conducted with randomly initialized variational parameters. However, recent works have shown that initializing the VQE using MP2 parameters (MP2-init-VQE) would improve the

VQE results substantially.[47] To understand the effect of the initialization on the accuracy, we performed additional calculations on the four-qubit UCCSD circuit of the H_2 molecule by initializing the VQE calculations with the MP2 parameters on a *noisy simulator*. By comparing the VQE results (Figure 4b) with MP2-init-VQE results (Figure S5a), we find that the MP2-init-VQE results are far superior to the VQE results, where changes up to 1.07 hartree are observed. However, as shown in Figure S5a, the DNNF predicted energies are more accurate than the MP2-init-VQE predicted energies, where the differences can be as high as 0.07 hartree (Figure S5b). Considering the average improvement of 0.03 hartree accuracy achieved with the DNNF compared to the MP2-init-VQE, we suggest using DNNF for computing ground state energies on the hardware.

Effect of Shot Count on the Accuracy of DNN-VQE Approaches on Noisy Simulators. To determine the effectiveness of four thousand shots in addressing the statistical noise, we considered an H_2 molecule at its equilibrium bond distance (0.735 Å), and computed its ground state energy using the DNN1, DNNF, and VQE methods by varying the shot counts from four thousand (4k) to ten thousand (10k), hundred thousand (100k), and five hundred thousand (500k), for all the four ansatzes (namely, the one-qubit, two-qubit, and four-qubit UCCSD, and the four-qubit Givens) on the *ibmq_qasm_simulator* with *ibm_brisbane* device noise and with the T-REx error mitigation. The results are listed in Figure 5. Although it is expected that a higher number of shots
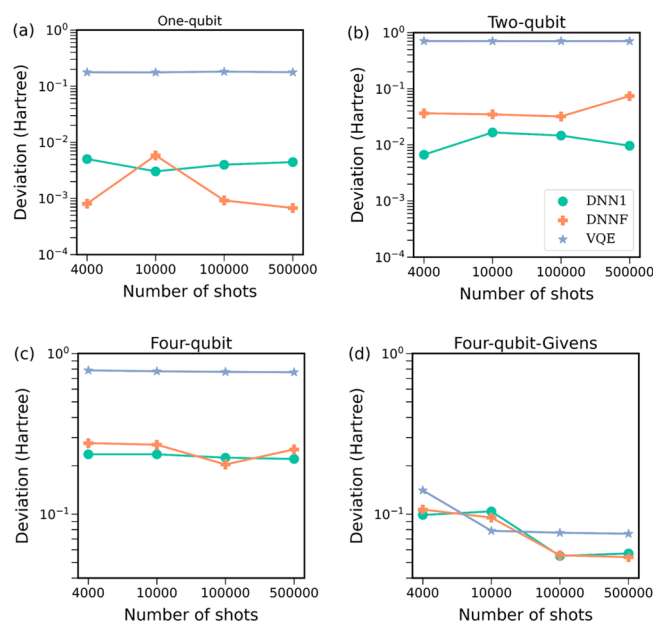

Figure 5. Deviations in the DNN1, DNNF, and VQE energies from the CCSD energy with an increase in the number of shots on a *noisy simulator* using (a) one-qubit UCCSD, (b) two-qubit UCCSD, (c) four-qubit UCCSD, and (d) four-qubit Givens circuits. All of the simulations were performed at an H−H bond distance of 0.735 Å.

should yield better accuracy, we did not find any such specific trends in our results (i.e., sometimes, a lower number of shots gave better accuracy). Moreover, across all the methods and ansatzes, the change in the energy with a variation in the shot count (between 4k to 500k) is less than 6%, with no specific trend. As such, these results indicate that, on a noisy simulator, the accuracy of the VQE and DNN-VQE approaches are
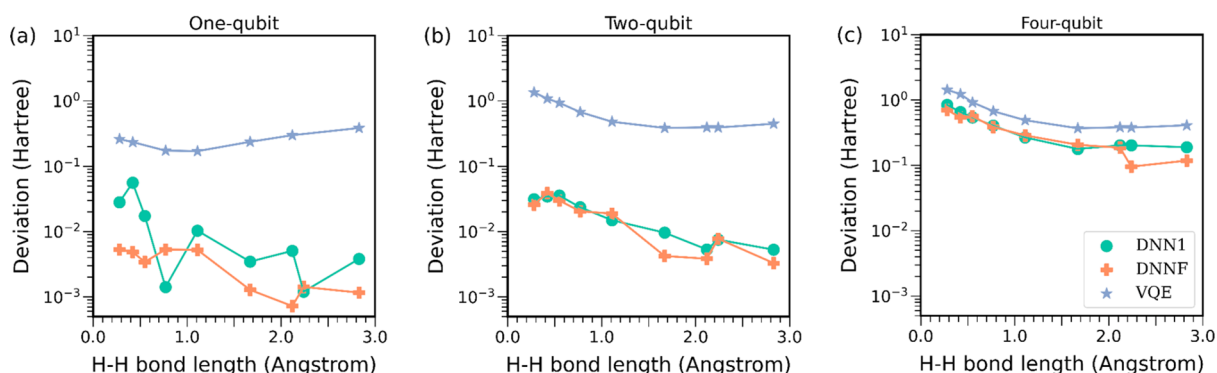
Figure 6. Deviation in the DNN1, DNNF, and VQE energies from the CCSD energy for an H_2 molecule represented using (a) one-qubit UCCSD, (b) two-qubit UCCSD, and (c) four-qubit UCCSD circuits. All the DNN1, DNNF, and VQE simulations were performed directly on the *ibm_brisbane* device (quantum computer) along with the T-REx error mitigation and four thousand shots.
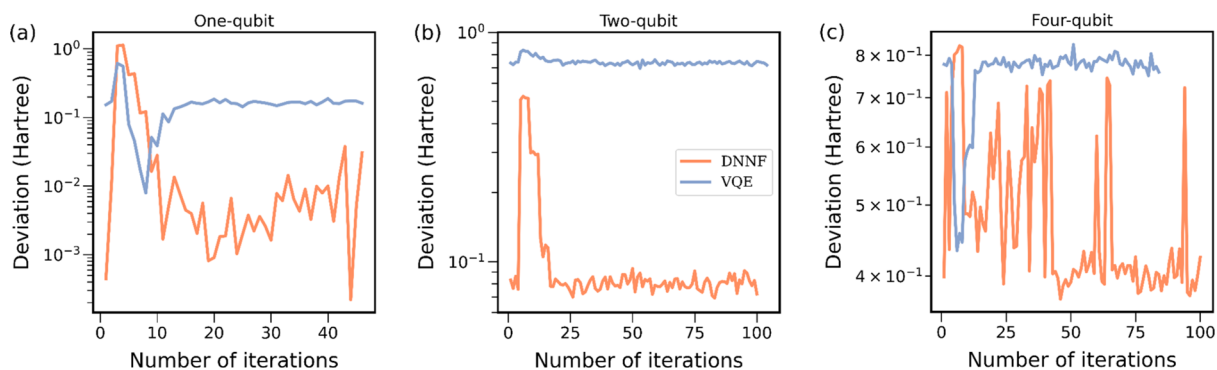

Figure 7. Deviation in the DNNF and VQE energies from the CCSD energy during the energy minimization of an H_2 molecule on the *ibm_brisbane* device along with T-REx error mitigation for (a) one-qubit, (b) two-qubit, and (c) three-qubit UCCSD circuits, and for an H—H bond distance of 0.77 Å.

roughly the same for shot counts between 4k to 500k. Considering this result and the fact that 4k shots are more manageable than larger shot counts on the current quantum devices, we conducted all our hardware calculations with 4k shots.

Hardware Results. To further check the reliability of the results obtained on noisy simulators, we conducted additional simulations on actual quantum computers. To this end, we computed the ground state energies of the H_2 molecules using DNN1, DNNF, and VQE methods on the *ibm_brisbane* device, along with T-REx error mitigation and 4k shots, for the one-, two-, and four-qubit UCCSD ansatzes. As illustrated in Figure 6, the results obtained on the real hardware follow the same trend as that of the *noisy simulator*. Even on the hardware, we observed that DNN methods provide more accurate energies than the VQE, and the accuracy of all methods decreases with an increase in the qubit count and circuit depth. Remarkably, for all three UCCSD circuits, the energy deviations of the DNN1, DNNF, and VQE from the CCSD are also roughly the same on the noisy simulators and hardware (where hardware results exhibit slightly higher deviations from the CCSD results than the results from the *noisy simulator*). Together, the hardware results not only validate the authenticity of the *noisy simulator* results but also reinforce the applicability of DNN1 and DNNF methods in determining the ground state energies of molecules on the state-of-the-art NISQ hardware.

Variation in the VQE and DNNF Predicted Energies on a Statevector Simulator, Noisy Simulator, and

Hardware. Since the energy minimization procedure using the DNNF method starts with the "DNN predicted" variational parameters, which closely correspond to the variational parameters of the ground state wave function obtained on a statevector simulator, it is expected that the DNNF energy would quickly reach the ground state energy than the VQE energy (for which the parameters will be initialized randomly). Indeed, our statevector results for the H_2 (for different circuits) and LiH molecules show that the DNNF energy converges in fewer iterations than the VQE energy (see Figure S6). Also, as shown in Figure S6, the DNNF (VQE) energy exhibits minimal (larger) deviation from the CCSD energy right from the first iteration due to its access to accurate (random) initial parameters. For the same reason, the DNN1 energies are quite accurate on a statevector simulator. Moreover, as noted in the earlier work,[35] the difference in the convergence speed becomes prominent as the number of parameters in the circuit increases. For example, the six-qubit LiH circuit, with ten parameters, took about 40 iterations for the DNNF and 90 for the VQE methods to converge their energies to a value that only deviates by 10^{-6} hartree from the CCSD energy.

Unfortunately, unlike the statevector results, we did not find any huge advantage in terms of speed for DNNF over VQE either on a *noisy simulator* (Figure S7) or on a hardware device (Figure 7). In both scenarios, although the DNNF energy at the first iteration is more accurate than the VQE energy, the presence of noise leads to only marginal improvements in accuracy for both DNNF and VQE energies as iterations

progress. Even after 100 iterations, DNNF and VQE energies show little change from their initial values, as observed with both the two and four-qubit UCCSD circuits of an H_2 molecule. Consequently, although DNNF shows a significant advantage over VQE in terms of accuracy, it does not provide any substantial improvement in terms of speed on current hardware devices. On the other hand, the DNN1 method proves to be extremely valuable since it provides energies that are as accurate as DNNF and at an impressive speed (since it is a single iteration method).

CONCLUSIONS AND OUTLOOK

In conclusion, we thoroughly investigated the potential of the DNN-VQE and VQE methods for estimating the ground state energies of molecules on contemporary quantum computers. To this end, we considered quantum circuits (ansatzes) of various depths and qubit counts, and conducted extensive simulations on the LiH and H_2 molecules, both in the presence and absence of device noise. After training the DNN models, we demonstrated the effectiveness of DNN-VQE approaches (DNN1 and DNNF) in accurately predicting the ground state energies of molecules on a noiseless statevector simulator, matching the accuracy of the standard VQE method. Next, by conducting simulations on a *noisy simulator* and real quantum hardware (*ibm_brisbane* device), we established that the DNN1 and DNNF predicted energies are far more accurate than the VQE energies, thereby highlighting the value of the DNN-VQE approaches in the presence of device noise. However, we also showed that as the qubit count and circuit depth increase, the accuracy of both VQE and DNN-VQE methods tends to decrease. Notably, we proved that although DNNF provides more accurate energies than VQE, it does not offer any advantage over VQE in terms of speed on current hardware devices, which DNN1 does. Overall, among the DNN1, DNNF, and VQE methods, we recommend using the DNN1 method on the current hardware devices for obtaining quick and accurate energies, and our recommendations are particularly effective for circuits of lower depth and fewer qubits.

To further enhance the accuracy of DNN-VQE approaches, exploring alternative, lower-depth ansatzes is essential. Such ansatzes can in turn be used to extend these methods to study larger molecular systems.[6,48,49] Similarly, exploring more sophisticated error mitigation techniques, such as zero noise extrapolation (ZNE) and probabilistic error correction (PEC), might reduce the effect of noise, and thereby, improve the accuracy of the DNN-VQE energies.[50−53] Additionally, the development of improved optimizers that are tailored for quantum hardware may provide better results.[54,55] As noted in our simulations, parameter optimization in the presence of noise is quite poor for both DNNF and VQE methods. In the absence of better optimizers and shallower circuits, the DNN1 method emerges as a preferred choice for the current quantum hardware since the quantum circuit is measured only for the given set of variational parameters, is independent of the optimizer, and demands fewer quantum computational resources.

ASSOCIATED CONTENT

ⓈⒾ Supporting Information

The Supporting Information is available free of charge at https://pubs.acs.org/doi/10.1021/acsomega.3c07364.

Effect of parameter initialization for the LiH molecule, details of the employed quantum circuits, DNN model layout, time taken to compute the energies on a *noisy simulator*, accuracy of various methods on a statevector simulator, comparison of DNNF and MP2-init-VQE results on a noisy simulator, convergence on a statevector simulator, variation of energies with number of iterations a noisy simulator, and deviation of various methods from the CCSD energies (PDF)

AUTHOR INFORMATION

Corresponding Author

Sharma S. R. K. C. Yamijala − *Department of Chemistry, Indian Institute of Technology Madras, Chennai 600036, India; Centre for Quantum Information, Communication, and Computing, Centre for Molecular Materials and Functions, and Centre for Atomistic Modelling and Materials Design, Indian Institute of Technology Madras, Chennai 600036, India;* ⓘ orcid.org/0000-0003-1773-9226; Email: yamijala@iitm.ac.in

Authors

Kalpak Ghosh − *Department of Chemistry, Indian Institute of Technology Madras, Chennai 600036, India; Centre for Quantum Information, Communication, and Computing, Indian Institute of Technology Madras, Chennai 600036, India;* ⓘ orcid.org/0000-0003-3646-6948

Sumit Kumar − *Department of Chemistry, Indian Institute of Technology Madras, Chennai 600036, India; Centre for Quantum Information, Communication, and Computing, Indian Institute of Technology Madras, Chennai 600036, India*

Nirmal Mammavalappil Rajan − *TCS Research, Tata Consultancy Services, Mumbai 400021, India*

Complete contact information is available at:
https://pubs.acs.org/10.1021/acsomega.3c07364

Author Contributions

Kalpak Ghosh: Conceptualization, Methodology, Software, Validation, Formal analysis, Investigation, Data curation, Writing−original draft, Writing−review and editing, Visualization. Sumit Kumar: Methodology, Data curation, Writing−review and editing. Nirmal R: Methodology, Writing−review and editing. Sharma S.R.K.C. Yamijala: Conceptualization, Methodology, Validation, Formal analysis, Resources, Writing−original draft, Writing−review and editing, Visualization, Supervision, Project administration, Funding acquisition.

Notes

The authors declare no competing financial interest.

from the Mphasis F1 foundation. We thank Dr. Manoj Nambiar, TCS research, Mumbai, for fruitful discussions.

■ REFERENCES

(1) McArdle, S.; Endo, S.; Aspuru-Guzik, A.; Benjamin, S. C.; Yuan, X. Quantum Computational Chemistry. *Rev. Mod. Phys.* **2020**, *92* (1), 015003.

(2) Aspuru-Guzik, A.; Dutoi, A. D.; Love, P. J.; Head-Gordon, M. Simulated Quantum Computation of Molecular Energies. *Science* **2005**, *309* (5741), 1704−1707.

(3) Abrams, D. S.; Lloyd, S. Simulation of Many-Body Fermi Systems on a Universal Quantum Computer. *Phys. Rev. Lett.* **1997**, *79* (13), 2586−2589.

(4) Peruzzo, A.; McClean, J.; Shadbolt, P.; Yung, M.-H.; Zhou, X.-Q.; Love, P. J.; Aspuru-Guzik, A.; O'Brien, J. L. A Variational Eigenvalue Solver on a Photonic Quantum Processor. *Nat. Commun.* **2014**, *5*, 4213.

(5) O'Malley, P. J. J.; Babbush, R.; Kivlichan, I. D.; Romero, J.; McClean, J. R.; Barends, R.; Kelly, J.; Roushan, P.; Tranter, A.; Ding, N.; Campbell, B.; Chen, Y.; Chen, Z.; Chiaro, B.; Dunsworth, A.; Fowler, A. G.; Jeffrey, E.; Lucero, E.; Megrant, A.; Mutus, J. Y.; Neeley, M.; Neill, C.; Quintana, C.; Sank, D.; Vainsencher, A.; Wenner, J.; White, T. C.; Coveney, P. V.; Love, P. J.; Neven, H.; Aspuru-Guzik, A.; Martinis, J. M. Scalable Quantum Simulation of Molecular Energies. *Phys. Rev. X* **2016**, *6* (3), 031007.

(6) Kandala, A.; Mezzacapo, A.; Temme, K.; Takita, M.; Brink, M.; Chow, J. M.; Gambetta, J. M. Hardware-Efficient Variational Quantum Eigensolver for Small Molecules and Quantum Magnets. *Nature* **2017**, *549* (7671), 242−246.

(7) Bian, T.; Murphy, D.; Xia, R.; Daskin, A.; Kais, S. Quantum Computing Methods for Electronic States of the Water Molecule. *Mol. Phys.* **2019**, *117* (15−16), 2069−2082.

(8) Google AI Quantum and Collaborators. Hartree-Fock on a Superconducting Qubit Quantum Computer. *Science* **2020**, *369* (6507), 1084−1089.

(9) Huggins, W. J.; O'Gorman, B. A.; Rubin, N. C.; Reichman, D. R.; Babbush, R.; Lee, J. Unbiasing Fermionic Quantum Monte Carlo with a Quantum Computer. *Nature* **2022**, *603* (7901), 416−420.

(10) Cao, Y.; Romero, J.; Olson, J. P.; Degroote, M.; Johnson, P. D.; Kieferová, M.; Kivlichan, I. D.; Menke, T.; Peropadre, B.; Sawaya, N. P. D.; Sim, S.; Veis, L.; Aspuru-Guzik, A. Quantum Chemistry in the Age of Quantum Computing. *Chem. Rev.* **2019**, *119* (19), 10856−10915.

(11) Bauer, B.; Bravyi, S.; Motta, M.; Kin-Lic Chan, G. Quantum Algorithms for Quantum Chemistry and Quantum Materials Science. *Chem. Rev.* **2020**, *120* (22), 12685−12717.

(12) Grimsley, H. R.; Economou, S. E.; Barnes, E.; Mayhall, N. J. An Adaptive Variational Algorithm for Exact Molecular Simulations on a Quantum Computer. *Nat. Commun.* **2019**, *10* (1), 1−9.

(13) Colless, J. I.; Ramasesh, V. V.; Dahlen, D.; Blok, M. S.; Kimchi-Schwartz, M. E.; McClean, J. R.; Carter, J.; de Jong, W. A.; Siddiqi, I. Computation of Molecular Spectra on a Quantum Processor with an Error-Resilient Algorithm. *Phys. Rev. X* **2018**, *8* (1), 011021.

(14) McClean, J. R.; Romero, J.; Babbush, R.; Aspuru-Guzik, A. The Theory of Variational Hybrid Quantum-Classical Algorithms. *New J. Phys.* **2016**, *18* (2), 023023.

(15) Romero, J.; Babbush, R.; McClean, J. R.; Hempel, C.; Love, P. J.; Aspuru-Guzik, A. Strategies for Quantum Computing Molecular Energies Using the Unitary Coupled Cluster Ansatz. *Quantum Sci. Technol.* **2019**, *4* (1), 014008.

(16) Tilly, J.; Chen, H.; Cao, S.; Picozzi, D.; Setia, K.; Li, Y.; Grant, E.; Wossnig, L.; Rungger, I.; Booth, G. H.; Tennyson, J. The Variational Quantum Eigensolver: A Review of Methods and Best Practices. *Phys. Rep.* **2022**, *986*, 1−128.

(17) Preskill, J. Quantum Computing in the NISQ Era and beyond. *Quantum* **2018**, *2*, 79.

(18) Jordan, P.; Wigner, E. Über das Paulische Äquivalenzverbot. *Eur. Phys. J. A* **1928**, *47* (9−10), 631−651.

(19) Tranter, A.; Sofia, S.; Seeley, J.; Kaicher, M.; McClean, J.; Babbush, R.; Coveney, P. V.; Mintert, F.; Wilhelm, F.; Love, P. J. The Bravyi-Kitaev Transformation: Properties and Applications. *Int. J. Quantum Chem.* **2015**, *115* (19), 1431−1441.

(20) Seeley, J. T.; Richard, M. J.; Love, P. J. The Bravyi-Kitaev Transformation for Quantum Computation of Electronic Structure. *J. Chem. Phys.* **2012**, *137* (22), 224109.

(21) Fedorov, D. A.; Peng, B.; Govind, N.; Alexeev, Y. VQE Method: A Short Survey and Recent Developments. *Materials Theory* **2022**, *6* (1), 1−21.

(22) Nielsen, M. A.; Chuang, I. L. *Quantum Computation and Quantum Information: 10th Anniversary ed.*; Cambridge University Press, 2010.

(23) Hatano, N.; Suzuki, M. Finding Exponential Product Formulas of Higher Orders. *Quantum Annealing and Other Optimization Methods* **2005**, *679*, 37−68.

(24) Barkoutsos, P. K.; Gonthier, J. F.; Sokolov, I.; Moll, N.; Salis, G.; Fuhrer, A.; Ganzhorn, M.; Egger, D. J.; Troyer, M.; Mezzacapo, A.; Filipp, S.; Tavernelli, I. Quantum Algorithms for Electronic Structure Calculations: Particle-Hole Hamiltonian and Optimized Wave-Function Expansions. *Phys. Rev. A* **2018**, *98* (2), 022322.

(25) Bharti, K.; Cervera-Lierta, A.; Kyaw, T. H.; Haug, T.; Alperin-Lea, S.; Anand, A.; Degroote, M.; Heimonen, H.; Kottmann, J. S.; Menke, T.; Mok, W.-K.; Sim, S.; Kwek, L.-C.; Aspuru-Guzik, A. Noisy Intermediate-Scale Quantum Algorithms. *Rev. Mod. Phys.* **2022**, *94* (1), 015004.

(26) Wecker, D.; Hastings, M. B.; Troyer, M. Progress towards Practical Quantum Variational Algorithms. *Phys. Rev. A* **2015**, *92* (4), 042303.

(27) McClean, J. R.; Boixo, S.; Smelyanskiy, V. N.; Babbush, R.; Neven, H. Barren Plateaus in Quantum Neural Network Training Landscapes. *Nat. Commun.* **2018**, *9* (1), 4812.

(28) Cerezo, M.; Sone, A.; Volkoff, T.; Cincio, L.; Coles, P. J. Cost Function Dependent Barren Plateaus in Shallow Parametrized Quantum Circuits. *Nat. Commun.* **2021**, *12* (1), 1791.

(29) Lee, J.; Huggins, W. J.; Head-Gordon, M.; Birgitta Whaley, K. Generalized Unitary Coupled Cluster Wave Functions for Quantum Computation. *J. Chem. Theory Comput.* **2019**, *15*, 311.

(30) Mondal, D.; Halder, D.; Halder, S.; Maitra, R. Development of a Compact Ansatz via Operator Commutativity Screening: Digital Quantum Simulation of Molecular Systems. *J. Chem. Phys.* **2023**, *159* (1), 014105.

(31) Halder, D.; Prasannaa, V. S.; Maitra, R. Dual Exponential Coupled Cluster Theory: Unitary Adaptation, Implementation in the Variational Quantum Eigensolver Framework and Pilot Applications. *J. Chem. Phys.* **2022**, *157* (17), 174117.

(32) Halder, D.; Halder, S.; Mondal, D.; Patra, C.; Chakraborty, A.; Maitra, R. Corrections beyond Coupled Cluster Singles and Doubles through Selected Generalized Rank-Two Operators: Digital Quantum Simulation of Strongly Correlated Systems. *J. Chem. Sci.* **2023**, *135* (2), 1−7.

(33) Rossmannek, M.; Pavošević, F.; Rubio, A.; Tavernelli, I. Quantum Embedding Method for the Simulation of Strongly Correlated Systems on Quantum Computers. *J. Phys. Chem. Lett.* **2023**, *14* (14), 3491−3497.

(34) Eddins, A.; Motta, M.; Gujarati, T. P.; Bravyi, S.; Mezzacapo, A.; Hadfield, C.; Sheldon, S. Doubling the Size of Quantum Simulators by Entanglement Forging. *PRX Quantum* **2022**, *3* (1), 010309.

(35) Tao, Y.; Zeng, X.; Fan, Y.; Liu, J.; Li, Z.; Yang, J. Exploring Accurate Potential Energy Surfaces via Integrating Variational Quantum Eigensolver with Machine Learning. *J. Phys. Chem. Lett.* **2022**, *13* (28), 6420−6426.

(36) Treinish, M. *Qiskit/qiskit-Metapackage: Qiskit 0.44.0*; Zenodo, 2023. DOI: 10.5281/ZENODO.2573505.

(37) Sun, Q.; Berkelbach, T. C.; Blunt, N. S.; Booth, G. H.; Guo, S.; Li, Z.; Liu, J.; McClain, J. D.; Sayfutyarova, E. R.; Sharma, S.; Wouters, S.; Chan, G. K.-L. P Y SCF: The Python-based Simulations

of Chemistry Framework. *Wiley Interdiscip. Rev. Comput. Mol. Sci.* **2018**, *8* (1), No. e1340.

(38) Hehre, W. J.; Stewart, R. F.; Pople, J. A. Self-Consistent Molecular-Orbital Methods. I. Use of Gaussian Expansions of Slater-Type Atomic Orbitals. *J. Chem. Phys.* **1969**, *51* (6), 2657−2664.

(39) Nation, P. D.; Treinish, M. Suppressing Quantum Circuit Errors Due to System Variability. *PRX Quantum* **2023**, *4* (1), 010327.

(40) Abadi, M.; Agarwal, A.; Barham, P.; Brevdo, E.; Chen, Z.; Citro, C.; Corrado, G. S.; Davis, A.; Dean, J.; Devin, M.; Ghemawat, S.; Goodfellow, I.; Harp, A.; Irving, G.; Isard, M.; Jia, Y.; Jozefowicz, R.; Kaiser, L.; Kudlur, M.; Levenberg, J.; Mane, D.; Monga, R.; Moore, S.; Murray, D.; Olah, C.; Schuster, M.; Shlens, J.; Steiner, B.; Sutskever, I.; Talwar, K.; Tucker, P.; Vanhoucke, V.; Vasudevan, V.; Viegas, F.; Vinyals, O.; Warden, P.; Wattenberg, M.; Wicke, M.; Yu, Y.; Zheng, X. TensorFlow: Large-Scale Machine Learning on Heterogeneous Distributed Systems. *arXiv* **2016**, No. 1603.04467v2.

(41) Kingma, D. P.; Ba, J. Adam: A Method for Stochastic Optimization. *arXiv* **2017**, No. 1412.6980v9.

(42) Fedorov, D. A.; Otten, M. J.; Gray, S. K.; Alexeev, Y. Ab Initio Molecular Dynamics on Quantum Computers. *J. Chem. Phys.* **2021**, *154*, 164103.

(43) Bravyi, S.; Gambetta, J. M.; Mezzacapo, A.; Temme, K. Tapering off Qubits to Simulate Fermionic Hamiltonians. *arXiv* **2017**, No. 1701.08213, (accessed 2023−08−21).

(44) Anselmetti, G.-L. R.; Wierichs, D.; Gogolin, C.; Parrish, R. M. Local, Expressive, Quantum-Number-Preserving VQE Ansätze for Fermionic Systems. *New J. Phys.* **2021**, *23* (11), 113010.

(45) Arrazola, J. M.; Di Matteo, O.; Quesada, N.; Jahangiri, S.; Delgado, A.; Killoran, N. Universal Quantum Circuits for Quantum Chemistry. *Quantum* **2022**, *6*, 742.

(46) van den Berg, E.; Minev, Z. K.; Temme, K. Model-Free Readout-Error Mitigation for Quantum Expectation Values. *Phys. Rev. A* **2022**, *105* (3), 032620.

(47) Halder, D.; Srinivasa Prasannaa, V.; Agarwal, V.; Maitra, R. Iterative Quantum Phase Estimation with Variationally Prepared Reference State. *Int. J. Quantum Chem.* **2023**, *123* (3), No. e27021.

(48) Gard, B. T.; Zhu, L.; Barron, G. S.; Mayhall, N. J.; Economou, S. E.; Barnes, E. Efficient Symmetry-Preserving State Preparation Circuits for the Variational Quantum Eigensolver Algorithm. *npj Quantum Information* **2020**, *6* (1), No. 10.

(49) Ganzhorn, M.; Egger, D. J.; Barkoutsos, P.; Ollitrault, P.; Salis, G.; Moll, N.; Roth, M.; Fuhrer, A.; Mueller, P.; Woerner, S.; Tavernelli, I.; Filipp, S. Gate-Efficient Simulation of Molecular Eigenstates on a Quantum Computer. *Phys. Rev. Appl.* **2019**, *11* (4), 044092.

(50) Temme, K.; Bravyi, S.; Gambetta, J. M. Error Mitigation for Short-Depth Quantum Circuits. *Phys. Rev. Lett.* **2017**, *119* (18), 180509.

(51) Giurgica-Tiron, T.; Hindy, Y.; LaRose, R.; Mari, A.; Zeng, W. J. Digital zero noise extrapolation for quantum error mitigation. *2020 IEEE Int. Conf. Quantum Comput. Eng. (QCE)* **2020**, 306 (accessed 2023-09-13).

(52) van den Berg, E.; Minev, Z. K.; Kandala, A.; Temme, K. Probabilistic Error Cancellation with Sparse Pauli-Lindblad Models on Noisy Quantum Processors. *arXiv* **2022**, No. 2201.09866v2, (accessed 2023−09−04).

(53) Halder, S.; Shrikhande, C.; Maitra, R. Development of Zero-Noise Extrapolated Projective Quantum Algorithm for Accurate Evaluation of Molecular Energetics in Noisy Quantum Devices. *J. Chem. Phys.* **2023**, *159* (11), 114115.

(54) Powell, M. J. D. A Direct Search Optimization Method That Models the Objective and Constraint Functions by Linear Interpolation. *Advances in Optimization and Numerical Analysis* **1994**, 51−67.

(55) Spall, J. C. an Overview of the Simultaneous Perturbation Method for Efficient Optimization. *Johns Hopkins Apl Technical Digest* **1998**, *19*, 482−492.

■ NOTE ADDED AFTER ASAP PUBLICATION

After this paper was published ASAP December 4, 2023, the manuscript type was changed from a Review to an Article. The corrected version was reposted December 8, 2023.